UDC 621.039

V. Borysenko, DSc,
V. Goranchuk,
A. Nosovskyi, DSc, Prof.
Institute for Safety Problems of Nuclear Power Plants of National Academy of Sciences (NAS) of Ukraine, 12 Lysogirska Str., Kyiv, Ukraine, 03028; e-mail: vborysenko@ispnpp.kiev.ua

DIAGNOSTICS OF IN-CORE NEUTRON MONITORING SYSTEM BASED ON ARTIFICIAL NEURAL NETWORK

В.І. Борисенко, В.В. Горанчук, А.В. Носовський. **Діагностика внутрішньозонного нейтронного контролю на основі застосування нейронних мереж.** Однією з задач діагностики внутрішньозонного нейтронного контролю є задача діагностики детекторів прямого заряду, а саме визначення достовірності сигналів, тобто визначення детектора прямого заряду якій відмовив. Важливо мати змогу оцінити енерговиділення в тепловидільній збірці з цим детектором прямого заряду. В статті обговорюються особливості відновлення сигналу детекторів прямого заряду на основі застосування технології нейронних мереж. Під відновленням сигналу відмовившиго детектора прямого заряду мається на увазі модельне відтворення сигналу, відсутнього через фізичне пошкодження детектора. Навчена нейронна мережа, на основі моніторингу вхідної інформації, може з високим ступенем точності передбачити появу дефектів в обладнанні й оцінити ступінь його технічного стану. Розглянуто мережі трьох різних архітектур: без прихованих шарів, з одним прихованим шаром та з двома прихованими шарами. На вхід нейронної мережі подавалися сигнали детекторів прямого заряду від різної кількості каналів нейтронних вимірювань – від 3 до 63, у якості вихідного сигналу слугували детектори прямого заряду каналів нейтронних вимірювань, що перевірявся. Моделювання було проведено для різних детекторів прямого заряду як за роком використання, так і за місцем розташування в активній зоні, а також для різних енергоблоків та паливних кампаній (26 та 27 кампанії ЗАЕС-5, 27 та 28 кампанії ХАЕС-1, 11 та 12 кампанії ХАЕС-2). Був досліджений вплив кількості вхідних сигналів, а також вплив кількості прихованих шарів на похибку визначення вихідного сигналу. Проведено порівняння алгоритмів навчання нейронних мереж: Левенберга-Марквардта та L-BFGS. Показана важливість вибору для нейронної мережі таких вхідних сигналів, що найбільше визначають характер вихідного сигналу. Показано, що відновлення сигналів детекторів прямого заряду можливе з похибкою не більше 2 % за умови навчання на широкому діапазоні даних, що дозволяє забезпечити контроль енергорозподілу в тепловидільній збірці з даним детектором прямого заряду.

Ключові слова: детектор прямого заряду, канал нейтронних вимірювань, система внутрішньореакторного контролю, нейронна мережа, діагностика систем, достовірність сигналів

V. Borysenko, V. Goranchuk, A. Nosovskyi. **Diagnostics of in-core neutron monitoring system based on artificial neural network.** One of the tasks of the diagnostics of in-core neutron control is the task of diagnostics of self-powered neutron detectors, namely the determination of reliability of self-powered neutron detectors signal, that is, the detection of the fault self-powered neutron detectors SPND. It is important to be able to estimate the power density in the fuel assembly with this self-powered neutron detector. The article discusses the features of the restoration of the self-powered neutron detectors signal based on the application of neural network technology. The restoration of the self-powered neutron detector signal means a model-based restoration of a signal that is not available due to physical damage of detector. A trained neural network, based on the monitoring of input information, can with a high degree of accuracy predict the appearance of defects in the equipment and assess the degree of its technical condition. The neural networks of three different architectures were considered: without hidden layers, with one hidden layer and two hidden layers. As the input of the neural network were taken self-powered neutron detectors signals from the various number of neutron flux measuring channels – from 3 to 63. As the output of the neural network were taken self-powered neutron detectors signals that were chosen for prediction. The simulation was carried out for different self-powered neutron detectors, both in terms of year of use and location in the core, as well as for different power units and fuel campaigns (26th and 27th fuel campaigns of ZNPP-5, 27th and 28th fuel campaigns of KhNPP-1, 11th and 12th fuel campaigns of KhNPP-2). The influence of the number of input signals, as well as the effect of the number of hidden layers on the error of the determination of the output signal, were investigated. A comparison of neuronal training algorithms (Levenberg-Marquardt and L-BFGS) was carried out. It is shown the importance of choosing such input signals for the neural network, which determine the nature of the output signal most. It is shown that the restoration of self-powered neutron detectors signals is possible with an error not more than 2%, provided neural network learning on a wide range of data, which allows to control the energy distribution in the fuel assembly with fault self-powered neutron detector.

Keywords: self-powered neutron detector, neutron flux measuring channel, in-core monitoring system, neural network, system diagnostics, signal reliability

Introduction

An in-core monitoring system is provided to control the distribution of energy in the VVER reactor core. This system provides the operator with operational information on energy release in the core based on the signals of self-powered neutron detectors (SPND) and coolant temperature sensors. The output signal of the SPND is proportional to the density of the neutron flux at its location, which in

DOI: 10.15276/opu.2.58.2019.04

ISSN 2076-2429 (print)
ISSN 2223-3814 (online)

turn also determines the energy release in the nearest fuel elements. In order to control the linear energy release of fuel when operating at rated power, it is necessary to ensure compliance with the regulatory requirements for the number of operational SPND. Detectors that malfunction should be detected in in-core monitoring system (ICMS) and be able to evaluate energy generation in a fuel assembly (FA) in which energy control was lost due to damage to the SPND or for other reasons.

Analysis of recent publications

The reliability of the input information in the ICMS was investigated in [1, 2]. In this article, the reliability of information that is defined in the ICMS is the property of information to be correctly perceived and uniquely interpreted for making management decisions. In [2], similar algorithms were used to analyze the reliability of the input information as in [1], but in real time. Estimates were performed on the basis of: analysis of statistical characteristics of channels, comparison with regime values and setpoints, comparison with information in parallel control channels [2]. At the same time, the technology of neural networks [3 – 5] showed its perspective for the analysis of the reliability of the input information of NPP control systems, which is considered in this paper in the problem of ICMS diagnostics.

The purpose and objectives of the study

The purpose of the study is to ensure the control of the reliability of the information of the measuring channels in the ICMS. The task of diagnosing SPND is to search for a failed SPND. This paper presents the results of a study on the possibility of model recovery of a failed SPND signal based on the use of neural network technology. When the signal of the failed SPND is restored, the model reproduces the signal missing due to physical damage to the detector.

How Neural Networks Work

Neural networks are a simplified model of the biological nervous system. They are used in solving classification and forecasting problems and can be applied to almost any task when there is a relationship between input variables and output (predicted), even when the relationship has a complex structure. A neural network is a collection of neural elements that are somehow connected to each other by relationships determined by weighting factors. The peculiarity of neural networks is that they are capable of learning. The learning process involves adjusting the weights.

The block diagram of the neuron model is presented in Fig. 1.

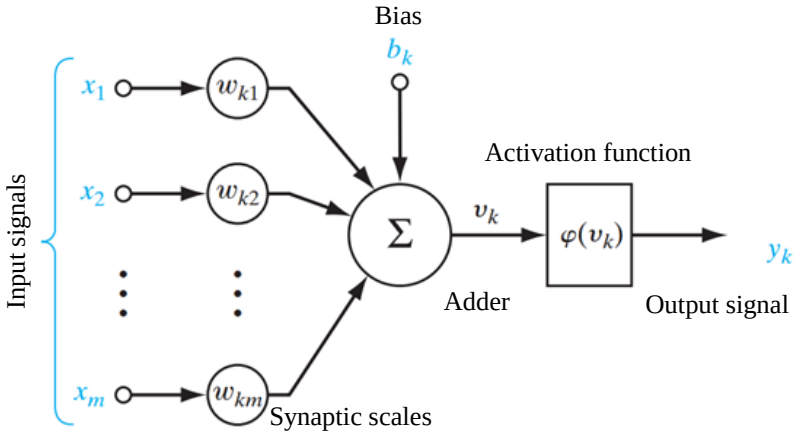

Fig. 1. Model of a neuron

Each synapse (ligament) is characterized by its weight. The signal x_j at the input of a synapse J that is associated with a neuron k is multiplied by weight ω_{kj}. The synaptic weight of the neuron can be both positive and negative.

The adder u_k sums the input signals weighted relative to the corresponding neuron synapses. An externally added offset may be included in the model of the neuron, denoted as b_k. The offset value b_k determines the decrease or increase of the input signal supplied to the activation function.

The activation function φ limits the amplitude of the output signal of the neuron. For example, the normalized range of neuron output amplitudes may lie in the range [0, 1] or [–1, 1]. Therefore, the model of the neuron is described by the following equations:

$$u_k = \sum_{j=1}^{m} \omega_{kj} x_j ,$$

$$v_k = u_k + b_k ,$$

$$y_k = \varphi(v_k) ,$$

where x_1, x_2, ..., x_m – input signals;

ω_{k1}, ω_{k2}, ..., ω_{km} – synaptic weights of the neuron k;

u_k – linear output combination of input signals;

b_k – bias;

v_k – activation potential;

$\varphi(v_k)$ – activation function;

y_k – the output signal of the neuron.

The neural network can be described using architecture and synaptic scales. There are three fundamental classes of architecture: single-layer direct distribution networks, multi-layer direct distribution networks, recurrent networks [6].

Modeling based on the use of neural network technology

The simulation was performed using the alglib cross-platform numerical analysis library [7]. The alglib library supports C ++, C #, Pascal, VBA, and Windows, Linux, Solaris. It used the C # programming language and the Windows operating system.

Neural networks were built with no hidden layers, with one hidden layer and two hidden layers. Network connections go from the input layer to the first hidden (if any), then to the second (if any), then to the original layer. Research on different neural network models was conducted to select the optimal neural network model.

Neural network training was conducted on the first five datasets and testing on the next fifteen. The time interval between the datasets was one week.

The simulation was performed for different SPND both by year of use and by location in the core area, as well as for different power units and fuel campaigns (26 and 27 ZNPP campaigns-5, 27 and 28 KhNPP campaigns-1, 11 and 12 KhNPP campaigns-2).

The influence of the number of input signals and the influence of the number of hidden layers on the error of determining the output signal was investigated. Comparison of learning algorithms of neural networks: Levenberg-Marquardt and L-BFGS.

Choosing the optimal neural network scheme for the recovery of SPND signals

The choice of the neural network scheme was performed according to the criterion of minimum deviation of the recovered SPND signal from the real SPND signal by 10 – 20 steps after simulating the fact of physical damage of the SPND.

The influence of the number of input signals.

On example 11 of the KhNPP-2 fuel campaign (see Fig. 2) three cases were considered (see Table 1): in the first calculation, the SPND signals from 63 NFMC were given, in the second calculation – from the 7 nearest NFMC (FA-137), FA-124, FA-111, FA-98, FA-99, FA-87, FA-88), in the third calculation – from 11 NFMC (FA-137, FA-154, FA-152, FA-129, FA-104, FA-50, FA-27, FA-10, FA-12, FA-35, FA-60), which were located in similar locations of the output NFMC in 30 ° symmetry sectors.

In all the considered cases, the current of the SPND NFMC-57, FA-114 served as the output signals (see Fig. 3). It is worth noting that the nearest neighboring NFMC to NFMC-57 is located through one fuel assembly, and FA-114 is located in the penultimate row – on the periphery of the core.

ISSN 2076-2429 (print)
ISSN 2223-3814 (online)

Table 1

Variation of the calculation from the actual value for the currents of SPND NFMC-57, KhNPP-2, 11th fuel campaign, depending on the number of input NFMC

№	The number of input NFMC	The number of output NFMC	Location of input NFMC in the core	The maximum deviation, %
1	63	1	All core	6.52
2	7		Near input NFMC	4.99
3	11		Symmetric across sector 30°	1.82

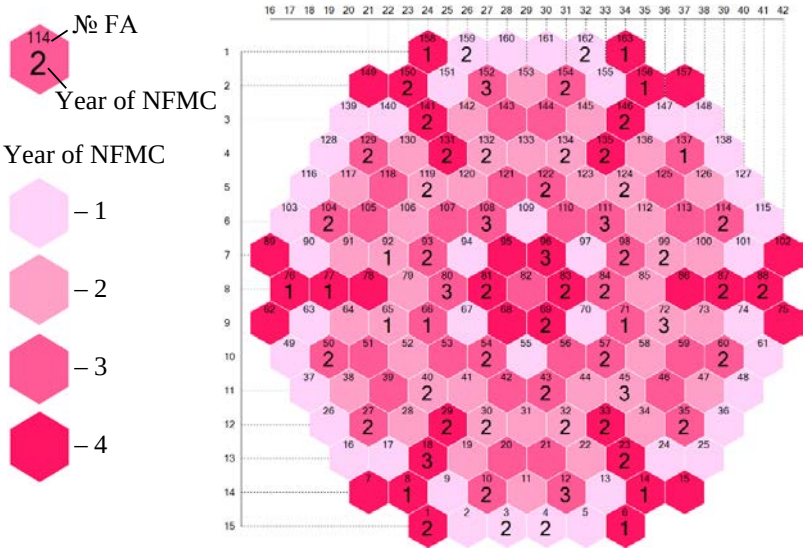

Fig. 2. Chartogram of the KHPP-2 11th fuel loading

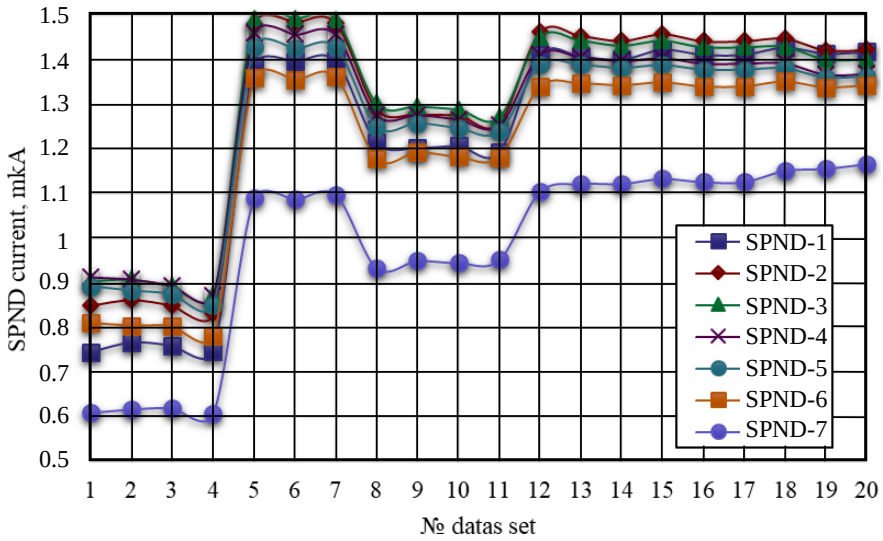

Fig. 3. Actual value of SPND NFMC-57 (FA-114) currents for the KhNPP-2 11th fuel campaign

Tables 2 – 4 present an error in the recovery of currents of the SPND NFMC-57 using neuralnetworks. The neural network architecture with no hidden layers was selected. The Levenberg-Marquardt algorithm was used to train neural networks. Training was conducted on the first five datasets and testing on the subsequent fifteen.

Table 2

The deviation of the calculated value of the current of the SPND from the actual according to item No. 1 of Table 1

№ set	Datas type	Deviation, %						
		SPND-1	SPND-2	SPND-3	SPND-4	SPND-5	SPND-6	SPND-7
1	Training	–0.02	–0.02	–0.02	–0.02	–0.02	–0.02	–0.02
2		–0.03	–0.03	–0.02	–0.02	–0.02	–0.01	–0.01
3		–0.02	–0.02	–0.02	–0.03	–0.04	–0.05	–0.06
4		–0.02	–0.02	–0.02	–0.02	–0.01	–0.01	0
5		–0.01	–0.01	–0.01	–0.01	–0.01	–0.01	–0.01
6	Test	–0.21	–0.1	–0.12	–0.25	–0.48	–0.44	–0.19
7		–0.21	–0.1	–0.31	–0.62	–1.03	–1.05	–1.01
8		–0.92	–0.15	–0.32	–1.04	–2.48	–2.63	–1.13
9		–0.62	0.07	–0.25	–1.08	–2.39	–2.71	–2.09
10		–0.82	0	–0.37	–1.31	–2.89	–3.2	–2.33
11		–0.71	0.1	–0.35	–1.34	–2.82	–3.17	–2.97
12		–0.72	–0.13	–0.51	–1.3	–2.42	–2.47	–2.32
13		–0.51	0.01	–0.55	–1.49	–2.61	–2.66	–3.35
14		–0.48	0.14	–0.56	–1.67	–2.93	–3.05	–3.88
15		–0.49	0.22	–0.62	–1.8	–3.31	–3.27	–3.95
16		–0.47	0.39	–0.61	–1.99	–3.67	–3.62	–4.23
17		–0.47	0.39	–0.61	–1.99	–3.67	–3.62	–4.23
18		–0.23	0.6	–0.64	–2.23	–3.96	–3.84	–5
19		0.32	1.15	–0.56	–2.66	–4.73	–4.51	–6.06
20		0.51	1.31	–0.58	–2.83	–4.97	–4.69	–6.52

Table 3

Deviation of the calculated value of the current of the SPND from the actual according to item No. 2 Table 1

№ set	Datas tape	Deviation, %						
		SPND-1	SPND-2	SPND-3	SPND-4	SPND-5	SPND-6	SPND-7
1	Training	–0.01	–0.03	–0.04	–0.04	–0.03	–0.02	0.01
2		–0.04	–0.05	–0.05	–0.04	–0.02	0	0.01
3		0	0.03	0.04	0.04	–0.02	–0.09	–0.16
4		–0.04	–0.05	–0.05	–0.04	–0.02	0.01	0.05
5		–0.01	–0.01	–0.01	–0.01	–0.01	–0.01	–0.01
6	Test	–0.3	–0.12	–0.07	–0.12	–0.23	–0.14	–0.01
7		–0.34	–0.1	–0.18	–0.34	–0.57	–0.56	–0.74
8		–1.53	–0.22	0.1	–0.18	–1.18	–1.4	–0.73
9		–1.19	0	0.13	–0.33	–1.27	–1.68	–1.78
10		–1.45	–0.08	0.06	–0.4	–1.48	–1.82	–1.79
11		–1.31	0	0.02	–0.55	–1.57	–1.96	–2.48
12		–1.12	–0.26	–0.31	–0.7	–1.24	–1.12	–1.48
13		–0.85	–0.14	–0.43	–0.96	–1.43	–1.2	–2.33
14		–0.86	–0.01	–0.37	–1.03	–1.59	–1.45	–2.81
15		–0.97	0.04	–0.4	–1.04	–1.75	–1.44	–2.78
16		–1.06	0.22	–0.27	–1.05	–1.92	–1.67	–3.09
17		–1.06	0.22	–0.27	–1.05	–1.92	–1.67	–3.09
18		–0.82	0.45	–0.26	–1.19	–2	–1.65	–3.69
19		–0.52	0.93	–0.03	–1.29	–2.23	–1.82	–4.58
20		–0.36	1.11	0	–1.35	–2.33	–1.86	–4.99

ISSN 2076-2429 (print)
ISSN 2223-3814 (online)

Table 4

The deviation of the calculated value of the current SPND from the actual according to item No. 3 Table 1

№ set	Datas tape	Deviation. %						
		SPND-1	SPND-2	SPND-3	SPND-4	SPND-5	SPND-6	SPND-7
1	Training	–0.01	0	–0.01	–0.01	0	0	0.01
2		–0.04	–0.04	–0.04	–0.03	0	0.03	0.03
3		–0.04	–0.05	–0.07	–0.1	–0.17	–0.22	–0.23
4		–0.01	0.01	0.02	0.04	0.08	0.1	0.1
5		–0.01	–0.01	–0.01	–0.01	–0.01	–0.01	–0.01
6	Test	–0.1	0.07	0.1	0.02	–0.07	0.03	0.28
7		–0.05	0.16	0.08	–0.03	–0.02	0.18	0.14
8		–0.55	0.32	0.36	–0.01	–0.61	–0.24	1.24
9		–0.38	0.36	0.26	–0.13	–0.42	–0.09	0.43
10		–0.53	0.4	0.29	–0.15	–0.61	–0.23	0.52
11		–0.45	0.41	0.23	–0.19	–0.36	0.12	0.16
12		–0.41	0.36	0.27	–0.05	–0.13	0.37	0.33
13		–0.28	0.44	0.24	–0.12	–0.02	0.56	–0.43
14		–0.33	0.52	0.26	–0.18	–0.03	0.57	–0.67
15		–0.39	0.63	0.28	–0.15	–0.15	0.62	–0.54
16		–0.45	0.74	0.29	–0.24	–0.2	0.68	–0.48
17		–0.45	0.74	0.29	–0.24	–0.2	0.68	–0.48
18		–0.44	0.85	0.3	–0.3	–0.1	0.86	–1.06
19		–0.31	1.19	0.45	–0.35	0.01	1.18	–1.52
20		–0.27	1.3	0.47	–0.37	0.06	1.31	–1.82

From the given data (Table 1) it is clear that the higher number of input signals of the neural network does not lead to better evaluation of the output signals. Therefore, we recommend that you limit yourself to only those inputs that most determine the output ones. A decrease in the number of NFMC inputs from 63 to 7 adjacent to the NFMC output resulted in a decrease of the maximum deviation of 1.53 %, and the use of NFMC inputs symmetrically located with the NFMC output in the 30° symmetry sectors resulted in a decrease in the maximum deviation by 3.17 %.

Investigation of the influence of the number of hidden layers

On the example of the KHPP-1 27th fuel campaign (see Fig. 4). three different neural network architectures (see Table 5) are considered: where no hidden layers, one hidden layer, and two hidden layers. The hidden layers included 20 neurons each.

Table 5

Deviation of calculation from actual value for SPND currents NFMC-2, KhNPP-1, 27th fuel loading, depending on the number of hidden layers

№	The number of input NFMC	The number of output NFMC	Location of input NFMC in the core	Number of hidden layers	Max deviation, %
1	3	1	symmetrical to the sector 30°	2	5.7
2				1	3.22
3				0	1.45

The output signal was the current of the SPND NFMC-2 (FA-81), and the output signal - NFMC in the sectors of symmetry 30 ° (FA-69, FA-83, FA-96). The actual values of the output signals are presented in Fig. 5. The neural network was trained by the Levenberg-Marquardt algorithm. Training was conducted on the first five datasets and testing on the subsequent fifteen.

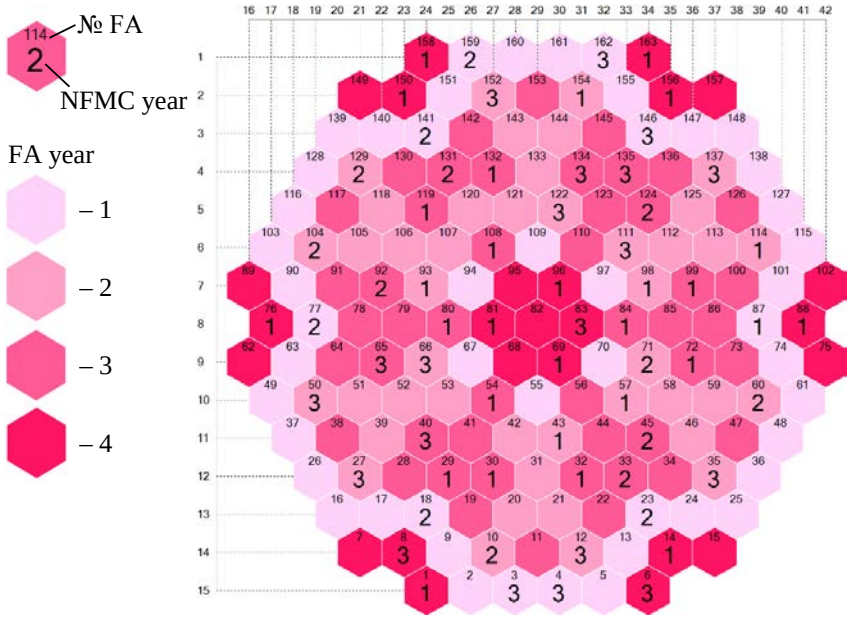

Fig. 4. Cartogram of the KHPP-1 27th fuel loading

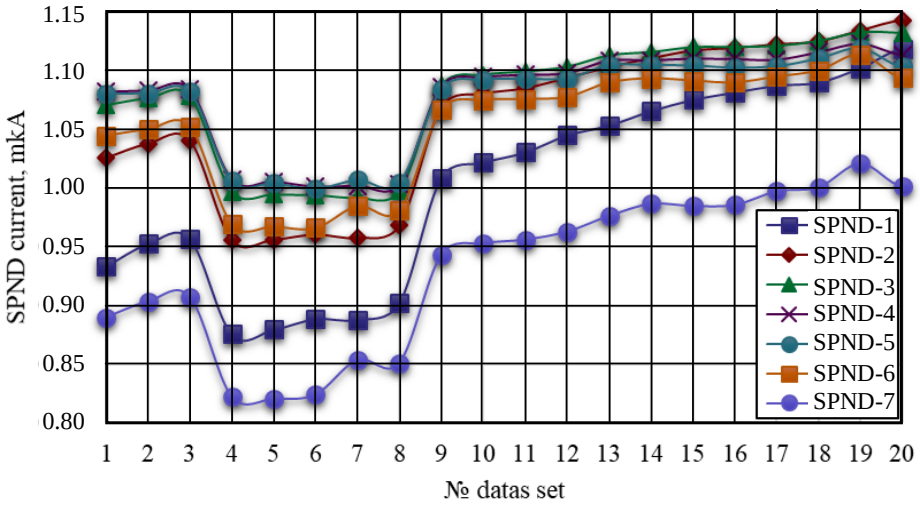

Fig. 5. Actual value of SPND NFMC-2 (FA-81) for the KHPP-1 27th fuel campaign

Higher number of hidden layers does not necessarily result in better evaluation of the output signals. It may be advisable to use neural networks without hidden layers to solve this problem. Thus, in this case, the neural network without hidden layers showed the maximum deviation of the calculated current of the SPND NFMC-2 from the actual level of 1.45 %, the neural network with one hidden layer – 3.22 %, and the neural network with two hidden layers – 5.7 %.

Comparison of neural network training algorithms

On the example of the 26th and 27th fuel campaigns of ZAES-5 (see Figs. 6, 7) there two algorithms for training neural networks (Levenberg-Marquardt and L-BFGS (see Table 6)) are considered. To the input of the neural network were signaled SPND from NFMC, which were in sectors of symmetry 30 ° similar to the original NFMC.

For the 26th fuel campaign. the signals of the SPND NFMC in FA-76, FA-150, FA-156, FA-88, FA-14 were fed to the input, and the SPND NFMC in FA-8 served as the output signal (see Fig. 8).

ISSN 2076-2429 (print)
ISSN 2223-3814 (online)

For the 27th fuel campaign, the signals of the SPND NFMC in FA 141, FA-146, FA-87, FA-23, FA-18 were fed to the input, and the SPND NFMC in FA-8 served as the output signal (see Fig. 9).

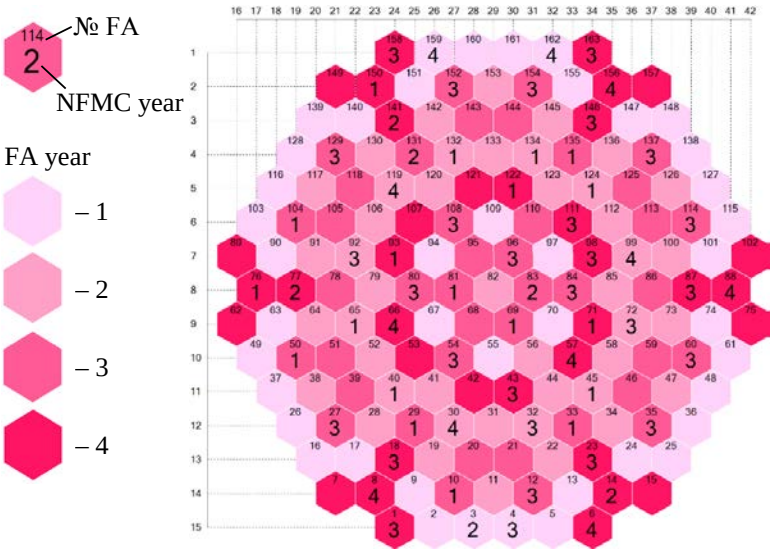

Fig. 6. Cartography of the 26th ZAES-5 fuel loading

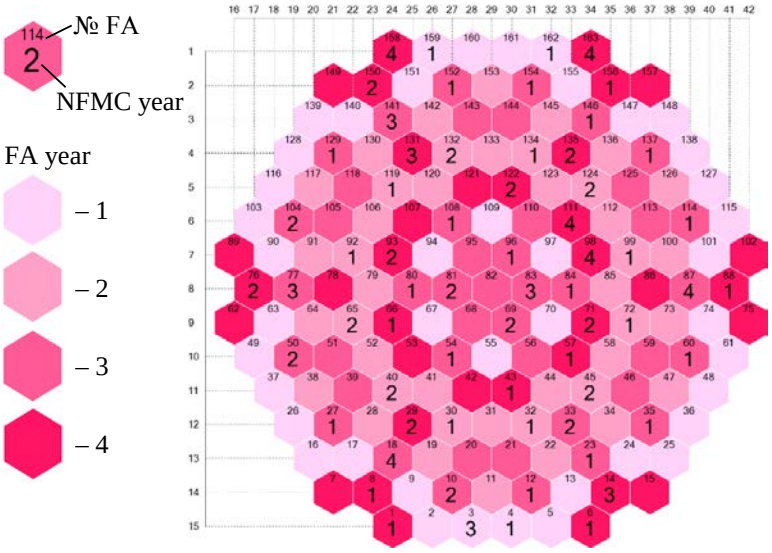

Fig. 7. Cartography of the 27th ZAES-5 fuel loading

Table 6

The deviation of the calculation from the actual value for the currents of the SPND ZAES-5 depending on the algorithm of training

№	Fuel campaign	№ FA	Algorithm of training	Max diviation, %
1	26	8	L-BFGS	5.47
2			Levenberg-Marquardt	1.66
3	27	77	L-BFGS	3.99
4			Levenberg-Marquardt	101.27

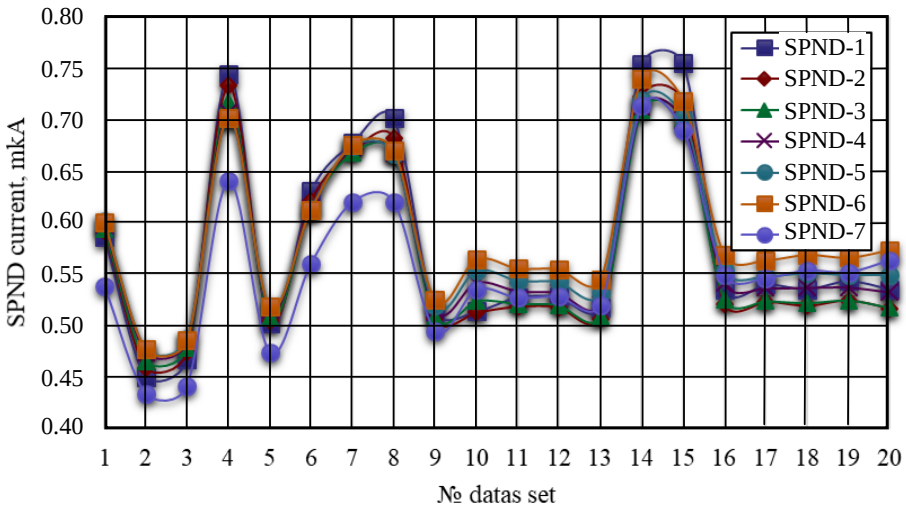

Fig. 8. Actual value of SPND NFMC-12 (FA-8) currents for the ZAES-5 26th fuel campaign

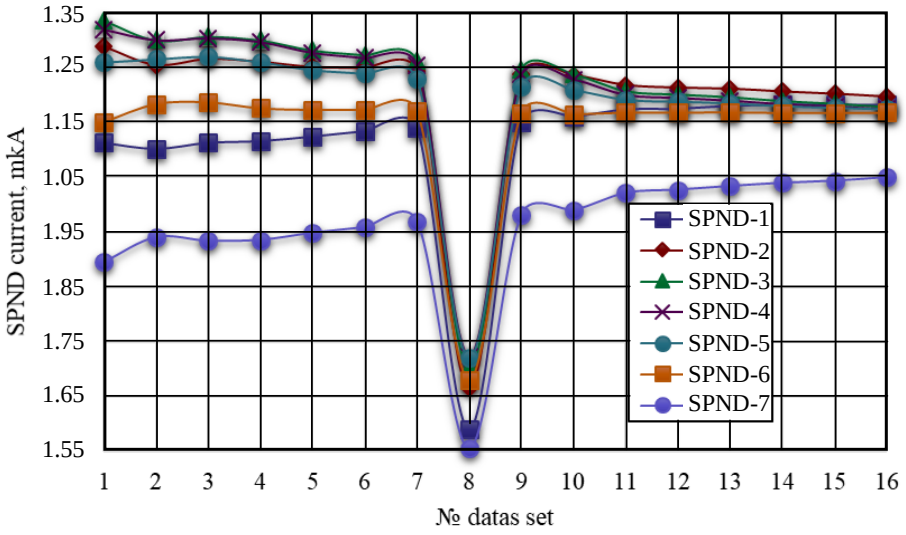

Fig. 9. Actual value of SPND NFMC-8 (FA-77) currents for the ZAES-5 27th fuel campaign

The neural network architecture with no hidden layers was selected. Training was conducted on the first five datasets. and testing on subsequent ones.

Fig. 7 presents the error of current recovery SPND NFMC-12 (FA-8) by the algorithm L-BFGS, and in Table, 8 according to the Levenberg-Marquardt algorithm for the ZAES-5 26th fuel campaign. As can be seen from the Table, 7, 8 Levenberg-Marquardt's training algorithm showed better recovery of DPF currents. This trend is observed for most calculations. although there are opposite cases.

It is worth noting that the current values of the SPND in the eighth data set are very different from those used in the training of the neural network.

As can be seen from the Table 9, 10, the L-BFGS training algorithm showed a much better recovery of SPND currents for the eighth data set. for other datasets with little advantage, the Levenberg-Marquardt algorithm turned out to be the best.

In the Table 9 presents the error of current recovery SPND NFMC-8 (FA-77) by the algorithm L-BFGS, and in Table 10 according to Levenberg-Marquardt algorithm for the ZAES-5 27th fuel campaign.

ISSN 2076-2429 (print)
ISSN 2223-3814 (online)

Table 7

The deviation of the calculated value of the current of the SPND from the actual according to item No. 1 of Table 6

№ set	Datas tape	Diviation, %						
		FA-1	FA-2	FA-3	FA-4	FA-5	FA-6	FA-7
1	Training	0.2	–0.39	0.1	–0.41	–0.04	0.06	0.77
2		0.75	0.34	–0.53	–0.41	0.04	–0.16	–0.3
3		–0.4	0.04	0.35	0.34	–0.26	0.17	–0.07
4		0.04	0.2	–0.06	0.12	–0.03	–0.04	–0.29
5		–0.68	–0.26	0.03	0.28	0.2	–0.1	–0.24
6	Test	–2.19	–0.47	1.28	1.35	–0.07	0.29	0.21
7		–1.3	–0.29	–0.15	0.24	0.71	–0.11	–0.06
8		–2.66	–0.68	0.87	1.58	0.46	–0.07	–0.54
9		–3.09	–0.55	–0.27	1.65	1.14	–0.13	–1.67
10		–2.53	–1.25	–2.82	0.12	2.51	–0.49	–2.05
11		–3.78	–1.8	–1.23	1.48	2.12	–0.52	–2
12		–4.14	–1.95	–1.26	1.65	2.13	–0.56	–2.2
13		–4.18	–1.89	–1.48	1.76	2.26	–0.66	–2.47
14		–4	–1.43	–2.09	1.34	2.45	–0.9	–3.14
15		–4.88	–1.32	–0.32	2.4	1.76	–0.58	–2.66
16		–5	–1.91	–1.7	1.98	2.88	–0.6	–2.82
17		–5.23	–1.75	–1.25	2.46	2.73	–0.67	–3.06
18		–5.29	–2.08	–2.1	2.2	3.18	–0.82	–3.35
19		–5.47	–1.81	–1.55	2.63	2.96	–0.73	–3.36
20		–5.42	–2.66	–3.19	2.16	3.8	–1.34	–4.16

Table 8

The deviation of the calculated value of the current of the SPND from the actual according to item No. 2 of Table 6

№ set	Datas set	Diviation, %						
		FA-1	FA-2	FA-3	FA-4	FA-5	FA-6	FA-7
1	Training	–0.01	–0.02	–0.02	–0.02	–0.03	–0.02	–0.01
2		0.02	–0.04	–0.04	–0.02	0	–0.02	–0.03
3		–0.05	–0.02	–0.02	–0.03	–0.04	–0.02	0
4		–0.02	–0.02	–0.02	–0.01	–0.01	–0.01	–0.02
5		–0.04	0	0	–0.02	–0.03	–0.03	–0.05
6	Test	–0.24	0.22	0.12	–0.1	–0.12	0.07	0.09
7		0.21	0.3	–0.1	–0.23	0.02	0.25	–0.32
8		–0.14	0.2	0.17	0.06	–0.06	–0.06	–0.12
9		0.36	0.05	0.1	0.28	0.25	0.02	–0.55
10		1.19	–0.29	–0.25	0.4	0.66	0.09	–1.24
11		0.6	–0.26	0.17	0.78	0.5	–0.28	–0.8
12		0.6	–0.34	0.14	0.84	0.48	–0.36	–0.9
13		0.64	–0.35	0.12	0.86	0.49	–0.38	–0.92
14		0.82	–0.33	–0.09	0.65	0.47	–0.44	–1.4
15		0.4	–0.06	0.14	0.5	0.19	–0.43	–1.04
16		1.14	–0.18	0.22	0.88	0.64	–0.14	–1.34
17		1.06	–0.07	0.36	1.03	0.59	–0.31	–1.27
18		1.27	–0.28	0.25	1.19	0.69	–0.35	–1.45
19		1.18	–0.13	0.35	1.14	0.63	–0.3	–1.36
20		1.54	–0.58	0.31	1.65	0.88	–0.76	–1.66

Table 9

The deviation of the calculated value of the current of the SPND from the actual according to item No. 3 of Table 6

№ set	Datas set	Diviation, %						
		FA-1	FA-2	FA-3	FA-4	FA-5	FA-6	FA-7
1	Training	0	–0.08	–0.09	–0.03	0.06	0.14	0.15
2		0.29	0.12	–0.03	–0.09	0	0.02	–0.24
3		–0.12	–0.13	0	0.02	–0.15	–0.23	0.22
4		–0.01	0.14	0.09	–0.01	–0.04	0	–0.04
5		–0.15	–0.05	0.04	0.11	0.13	0.08	–0.09
6	Test	–0.32	–0.21	–0.01	0.16	0.22	0.15	–0.12
7		–0.41	–0.33	–0.07	0.25	0.37	0.27	–0.24
8		3.99	3.64	2.11	0.95	0.73	2.58	2.09
9		–0.65	–0.69	–0.18	0.33	0.52	0.32	–0.4
10		–0.89	–0.84	–0.22	0.34	0.63	0.41	–0.41
11		–1.29	–1.21	–0.49	0.31	0.88	0.62	–0.71
12		–1.35	–1.22	–0.54	0.32	0.96	0.74	–0.76
13		–1.48	–1.3	–0.61	0.31	1	0.81	–0.78
14		–1.6	–1.34	–0.67	0.29	1.09	0.9	–0.86
15		–1.61	–1.35	–0.71	0.29	1.14	0.96	–0.91
16		–1.63	–1.37	–0.78	0.24	1.17	1.05	–1.03

Table 10

The deviation of the calculated value of the current of the SPND from the actual according to item No. 4 of table 6

№ set	Datas set	Diviation, %						
		FA-1	FA-2	FA-3	FA-4	FA-5	FA-6	FA-7
1	Training	–0.02	–0.02	–0.02	–0.02	–0.02	–0.02	–0.02
2		–0.02	–0.02	–0.02	–0.02	–0.02	–0.02	–0.02
3		–0.02	–0.02	–0.02	–0.02	–0.02	–0.02	–0.02
4		–0.02	–0.02	–0.02	–0.02	–0.02	–0.02	–0.02
5		–0.02	–0.02	–0.02	–0.02	–0.02	–0.02	–0.02
6	Test	–0.01	–0.05	–0.13	–0.13	–0.01	0.02	–0.39
7		0.01	–0.02	–0.18	–0.19	–0.02	0.07	–0.68
8		–13.34	11.86	34.09	26.83	–9.38	–4.09	101.27
9		–0.07	–0.12	–0.2	–0.26	–0.08	0	–0.89
10		–0.13	–0.13	–0.29	–0.41	–0.07	0.06	–1.17
11		–0.37	–0.15	–0.5	–0.73	–0.15	0.15	–1.63
12		–0.44	–0.14	–0.54	–0.75	–0.12	0.24	–1.61
13		–0.49	–0.15	–0.65	–0.87	–0.14	0.28	–1.81
14		–0.61	–0.15	–0.68	–0.92	–0.14	0.31	–1.8
15		–0.66	–0.14	–0.69	–0.93	–0.15	0.33	–1.77
16		–0.73	–0.16	–0.74	–0.99	–0.2	0.36	–1.79

Therefore. a neural network using the L-BFGS algorithm showed a better ability to generalize, that is, to return the correct result based on data that did not participate in the training sample.

For a good recovery of SPND currents it is necessary to train a neural network on a wide range of data. Also, do not seek to minimize the error in training the network. as the network can be converted and lose its ability to generalize.

Conclusions

The results of the calculations showed the suitability of the use of neural networks for the diagnosis of in-core neutron control. Recovery of SPND signals has been shown to be possible with a deviation of no more than 2 % provided that the neural network is trained over a wide range of data. This makes it possible to determine the current of the SPND that has failed, and also allows the control of the energy distribution in the fuel assembly even with the failed SPND.

ISSN 2076-2429 (print)
ISSN 2223-3814 (online)

The best results from the SPND signal recovery were obtained using the Levenberg-Marquardt training algorithm. The L-BFGS algorithm showed better speed than the Levenberg-Marquardt algorithm.

A neural network with no hidden layers has been identified as having the best architect. The importance of choosing for the neural network such input signals that most determine the nature of the output signal is shown.

Thus, when fed to the input of the neural network of SPND signals in the sectors of symmetry 30° to the output signal error was 3…4 times smaller than the case when the input signals were given to all SPND core. For a more accurate restoration of the currents of the SPND, it is necessary to train the neural network over a wide range of data.

Література

1. Саунин Ю.В., Добротворский А.Н., Семенихин А.В. Специализированное программное обеспечение для проведения комплексных испытаний системы внутриреакторного контроля реакторов ВВЭР. *Обеспечение безопасности АЭС с ВВЭР*. сб. тезисов докладов VI Междунар. научн.-технич. конф. Подольск. ОКБ Гидропресс, 26-29 мая 2009 г. 105 с.
2. Семенихин А.В., Саунин Ю.В., Жук М.М. Опробование системы диагностики входной информации СВРК на энергоблоке №1 Нововоронежской АЭС-2. *Известия вузов. Ядерная энергетика*. 2017. № 3. С. 88–95.
3. Messai A., Mellit A., Abdellani I., Massi P.A. On-line fault detection of a fuel rod temperature measurement sensor in a nuclear reactor core using ANNs. *Progress in Nuclear Energy*. March 2015. Vol. 79. P. 8–21.
4. Pirouzmand A., Dehdashti M.K. Estimation of relative power distribution and power peaking factor in a VVER-1000 reactor core using artificial neural networks. *Progress in Nuclear Energy*. November 2015. Vol. 85. P. 17–27.
5. Борисенко В.І., Горанчук В.В. Використання технології нейронних мереж для відновлення сигналів детекторів, які вийшли з ладу. *Проблеми безпеки атомних станцій і Чорнобиля.* Чорнобиль. 2018. Вип. 30. С. 17–23.
6. Haykin S. Neural networks and learning machines. Third Edition. Upper Saddle River. New Jersey : Pearson Education, 2009. 936 p.
7. ALGLIB-C++/C# numerical analysis library. URL: www.alglib.net (дата звернення 10.04.2019).

References

1. Saunin, Yu.V., Dobrotvorskiy, A.N., Semenikhin A.V. (2009). Specialized software for complex testing of the in-core monitoring system of VVER reactor. Safety assurance of NPP with VVER. *Proceding of 6th international scientific and technical conference (May 26-29).* Podolsk: OKB Gidropress. 105.
2. Semenikhin A.V., Saunin Yu.V., Zhuk M.M. (2017). Testing of the in-core monitoring system input data at unit № 1 of Novovoronezh NPP-2. *Izvestiya vuzov. Yadernaya Energetika, 3,* 88 – 95.
3. Messai, A., Mellit, A., Abdellani, I., Massi, P.A. (2015). On-line fault detection of a fuel rod temperature measurement sensor in a nuclear reactor core using ANNs. *Progress in Nuclear Energy, 79,* 8–21.
4. Pirouzmand, A., Dehdashti, M.K. (2015). Estimation of relative power distribution and power peaking factor in a VVER-1000 reactor core using artificial neural networks. *Progress in Nuclear Energy, 85,* 17–27.
5. Borysenko, V.I., Goranchuk, V.V. (2018). Use of neural network technologies to recover failed detector signal. *Problems of nuclear power plants safety and of Chornobyl,* 30, 17–23.
6. Haykin, S. (2009). *Neural networks and learning machines. Third Edition.* Upper Saddle River. New Jersey: Pearson Education. 936.
7. ALGLIB - C++/C# numerical analysis library. (2019. April 15) Retrieved from: http://www.alglib.net.

Борисенко Володимир Іванович; Borysenko Volodymyr, ORCID http://orcid.org/ 0000-0002-3035-0760
Горанчук Вадим Вікторович; Goranchuk Vadym, ORCID https://orcid.org/0000-0002-1505-2749
Носовський Анатолій Володимирович; Nosovskyi Anatolii, ORCID http://orcid.org/ 0000-0002-2594-3780

Received April 02, 2019
Accepted September 03, 2019